Liquid-crystalline poly(azomethine)s: 2. Structural formation kinetics

Stephen Z. D. Cheng, James J. Janimak, Tim M. Lipinski, Krishnamurthy Sridhar, Xiao Yan Huang and Frank W. Harris

Institute and Department of Polymer Science, College of Polymer Science and Polymer Engineering, The University of Akron, Akron, Ohio 44325, USA

(Received 17 April 1989; revised 12 June 1989; accepted 8 July 1989)

Characterization of the structural formation kinetics in a series of liquid-crystalline poly(azomethine)s (PAMEs), containing different numbers (n) of ethylene glycol flexible spacers, has been investigated. It has been previously established that, after crystal melting, all PAMEs demonstrate a nematic liquid-crystalline phase, prior to their isotropic melts. The polymers only exhibit liquid-crystalline glassy phases after quenching ($n=1$) or on cooling ($n=2$, 3 and 4). The isotropic to nematic transitions for PAMEs($n=2$, 3 and 4) proceed by two processes: a fast process followed by a slow structure-sensitive process achieved only on annealing isothermally. Both the fast and the slow processes are greatly influenced by the number of flexible spacers. The fast process is closely associated with a texture of high disclination density, whereas the slow process involves transformations of disclination. Isothermal experiments in the sub-T_g region reveal that the enthalpy relaxations for quenched samples from the nematic and isotropic states are different in the initial stages. The kinetics of this relaxation phenomenon has also been discussed.

(Keywords: crystal; enthalpy relaxation; glass transition; isotropic; kinetics; liquid-crystalline glass; liquid crystal; nematic, poly(azomethine); sub-T_g annealing; structure recovery; texture)

INTRODUCTION

Main-chain mesogen-non-mesogen liquid-crystalline poly(azomethine)s (PAMEs) have been synthesized recently[1,2] with systematic variations in the numbers of both mesogenic groups and flexible spacers. The thermodynamic properties of a new series of PAMEs containing different numbers (n) of ethylene glycol flexible spacers ($n=1$, 2, 3 and 4) have been reported in the preceding paper[3]. After crystal melting, all PAMEs show nematic liquid-crystalline phases before they reach their isotropic melts. The polymers can form single liquid-crystalline (LC) glassy states after quenching ($n=1$) or on cooling ($n=2$, 3 and 4). In a wide temperature range of 230–620 K, the heat capacities of the polymers in solids, nematic liquid crystals and isotropic melts have been measured. Pre-glass transitions of the PAMEs have been distinguished in lower-temperature regions, and they are attributed to the contributions of flexible spacers. Both transitions from rigid crystals to nematic liquid crystals (C/N) and from nematic crystals to isotropic melts (N/I) were reported, and their enthalpy and entropy changes during the transitions were also discussed. The thermodynamic data of the transitions for the PAMEs are listed in *Table 1*.

In this paper, the second paper in this series, we will report our experimental observations of structural formation kinetics of the transitions in the PAMEs. This includes studies of both first-order transitions and glass transitions of the PAMEs. In the first-order transitions, for PAME($n=1$), the transition between its rigid crystal and nematic liquid crystal (C/N) is investigated. For PAME($n=2$, 3 and 4), on the other hand, we focus on transitions between their nematic liquid crystals and isotropic melts (N/I). From our observations, we can clearly demonstrate the characteristic difference between the kinetics of C/N and N/I transitions. The kinetics of the N/I transitions have been studied very little in depth[4]. Generally, these transitions take place so quickly that it is difficult to identify any kinetic influence. It has been commonly claimed that the N/I transition is of equilibrium nature. However, studies of the N/I transition for some small molecules, such as cholesteryl acetate, myristate, nonanoate and esters, have shown a fit to Avrami kinetics[5,6], which indicates that they follow nucleation and growth steps. Our investigation reveals that, in liquid-crystalline PAMEs, the kinetics of N/I transition is certainly different from the transition behaviour of small molecules, but this is mainly a reflection of aggregation and annealing kinetics.

In the LC glass transition region, special attention is given to the enthalpy relaxation ('structure recovery' proposed by Kovacs *et al.*[7] in a semiquantitative phenomenological order-parameter model) of the PAMEs. It is also evident that such relaxation behaviour appears in polymeric amorphous glasses, such as polystyrene[8–12], poly(methyl methacrylate)[11,13,14], poly(vinyl acetate)[11], poly(ethylene terephthalate)[9] and poly(vinyl chloride)[13,15,16], and copolymers[14,16].

The enthalpy lost on annealing after a certain period of time at a particular annealing temperature within the LC glass transition is very much non-linear and dependent on thermal history. The rate of enthalpy recovery in non-equilibrium PAME LC glasses is faster for the samples quenched from their isotropic states compared to those quenched from their nematic states in the initial period of time. At prolonged annealing times, their relaxation processes become identical. An explanation has been attempted.

0032-3861/90/061122-08
© 1990 Butterworth-Heinemann Ltd.

Table 1 Thermal properties of PAMEs in the glass transitions and first-order transitions measured on heating at 10 K min^{-1}

PAMEs (n)	T_g (K)	ΔC_p (J K^{-1} mol^{-1})	T_d (K)	ΔH_d (kJ mol^{-1})	T_i (K)	ΔH_i (kJ mol^{-1})
1	350	137.3	534.7	20.2	?[a]	?[a]
2	318	173.9	439.8	13.0	566.4	2.0
3	305	199.7	416.0	21.7	502.8	2.1
4	293	234.4	368.3	12.3	467.0	2.3

[a] For PAME($n=1$) T_i is higher than its decomposition temperature, and thus it cannot be determined

EXPERIMENTAL

Differential scanning calorimetry

D.s.c. measurements were done on a Perkin–Elmer DSC2, which has been interfaced with an IBM XT computer and a software package developed by Microsystems Inc. Temperature and heat-capacity calibrations were performed following standard procedures with high-purity, sharp-melting substances (n-dodecane, naphthalene, benzoic acid, indium, lead and tin) over a wide range of heating rates[17]. All tests were conducted under a dry nitrogen atmosphere, with rates of 40–60 ml min^{-1}. For the measurements of heat capacity, the baselines of the empty pan and sapphire reference were measured and compared with the heat-flow measurements of the PAME samples. The PAMEs were enclosed in hermetic aluminium pans. The weights of the samples and the pans were controlled to within ± 0.002 mg. Sample weights were in the range 15–20 mg for heat-capacity and isothermal measurements, and 4–15 mg for non-isothermal measurements, depending upon heating or cooling rates. The heat-capacity runs were performed in three selected temperature ranges: from 220 K to below T_g for the solid heat capacity and T_g region measurements; T_g to above T_i; and above T_i to below the decomposition temperature for measurements of heat capacity in the nematic and liquid states. The DSC2 was calibrated in these three temperature ranges following standard procedures[17].

Isothermal experiments were conducted by heating the specimens to a temperature of 10 K above their equilibrium transition temperatures at 10 K min^{-1} (T_i for $n=2$, 3 and 4 and T_d for $n=1$), maintaining them at that temperature for 1 min and then quenching to preselected temperatures for a set predetermined time. The specimens were then reheated without prior cooling, and the heating traces were recorded. Peak temperatures were assigned as the temperatures of the transitions. The half-widths of the peaks were measured as the widths of the peaks at half-height, $\Delta T(1/2)$. Non-isothermal experiments were performed by heating the specimens to above the transition temperature at 10 K min^{-1}. Then the specimens were cooled at various rates, and the cooling traces were recorded. The samples were immediately reheated at a heating rate identical to the cooling rate, in order to eliminate possible reorganization or pre-melting effects. Besides the peak temperatures, the onset starting temperatures were also recorded for both cooling and heating processes. On cooling, the onset starting temperature is defined as the intersection between baseline and extrapolation of peak line at the high-temperature side, T_c(onset). On heating, on the other hand, the onset temperature is determined by the intersection between baseline and extrapolation of peak line at the low-temperature side, T_d(onset).

Structural recovery experiments were performed on three of the PAMEs ($n=2$, 3 and 4). The samples were annealed at a temperature within the glass transition region but below their respective glass transitions for various predetermined times (t_a) through quenching from their liquid-crystalline states. The annealing temperatures were chosen at 295 and 303 K for PAME($n=2$), 250 K for PAME($n=3$) and 273 K for PAME($n=4$). After annealing, the samples were heated up to a temperature 50 K above their glass transition temperatures at 10 K min^{-1} and the heating traces were recorded. The enthalpy change on annealing after time t_a (minutes) at an isothermal temperature of T_a (K) will be denoted as $\Delta H(t_a, T_a)$ in this paper. The values of $\Delta H(t_a, T_a)$ were calculated by integration of the difference between the heat capacity of the annealed samples and that of the unannealed one, represented as:

$$C_p(T)=[C_{p,ann}(T)-C_{p,unann}(T)]$$

Reproducibility was ensured by repeating the measurement of $\Delta H(t_a, T_a)$ at the same annealing time twice.

In order to compare the thermal history effects caused by their initial states, a set of parallel experiments were performed by quenching the PAMEs($n=2$, 3 and 4) from their isotropic states. The previous experimental conditions were repeated.

Polarized optical microscopy

A polarized optical microscope (Nikon Labophot-pol) was used in conjunction with a Mettler hot stage (Mettler FP-52). The specimens were immediately transferred from their isotropic melts to a preselected isothermal temperature, T_c, below their isotropization temperature, T_i. Thermal equilibrium was usually reached within 5–15 s prior to measurement. Measurement of the average birefringent light intensity was via a photosensitive light-meter attached to the microscope column. In order to study the liquid-crystalline textures, photographs were taken with a 35 mm camera. Finally, the hot stage was calibrated with standard, sharp-melting substances. Its temperature control was better than ± 0.2 K. The annealing time was recorded by a timer.

RESULTS

Kinetics of N/I transitions

Isothermal experiments. Figures 1 and *2* illustrate the effects of various isothermal temperatures and times on the I/N transition of PAME($n=3$), as an example. *Figure 1* shows the relationship between the half-widths of the transition peaks and annealing time. It is apparent that the half-widths decreases logarithmically with increasing annealing time at different isothermal temperatures. This effect becomes increasingly pronounced as the isothermal temperature is increased. At the same time,

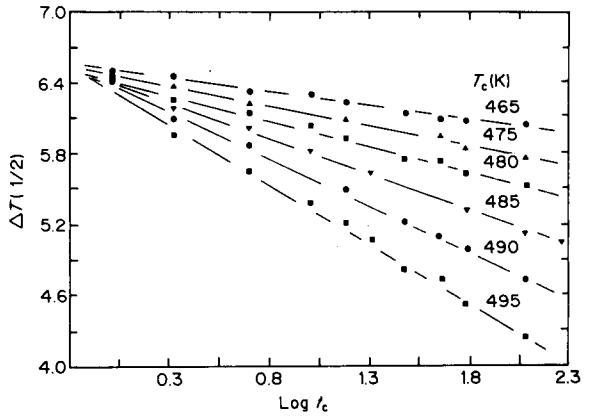

Figure 1 Relationship between the peak half-widths of the I/N transitions and logarithmic annealing time for PAME($n=3$) at different isothermal temperatures

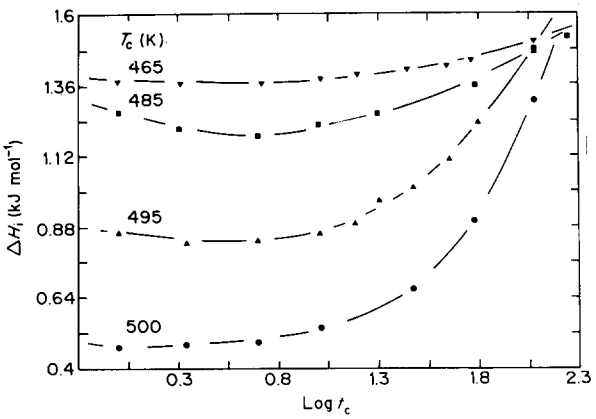

Figure 2 Relationship between the enthalpies of the I/N transitions and logarithmic annealing time for PAME($n=3$) at different isothermal temperatures

on the other hand, although the transition temperatures in this study have a tendency to increase slightly with isothermal temperature and time, they are still within the experimental uncertainty (±2 K). In *Figure 2*, one observes that the enthalpies of transition also become dependent upon isothermal temperature and time. Of special interest is that, at a low isothermal temperature (465 K), the enthalpy of transition of PAME($n=3$) remains almost constant with respect to time. With increasing isothermal temperature, one can find an initial decrease in the enthalpy of transition at very short time periods (within 1 min), and this is followed by a gradual increase in the enthalpy of transition at longer time periods (up to 3 h).

A similar observation has been observed in the case of PAME($n=4$) above an isothermal temperature of 430 K. Below 430 K, the enthalpies of transition are almost constant with respect to both temperature and time.

Through the polarized optical microscope (p.o.m.) observation of PAME($n=3$ and 4), one can semi-quantitatively follow the I/N transition behaviour related to the intensity change of birefringence even at short time periods (say about a few seconds). As shown in *Figure 3*, which plots the relationship between the difference in birefringence of the PAME($n=3$) at two temperatures (475 and 495 K) and logarithmic time, a very rapid increase in the change of birefringence is initially observed in a time period of a few seconds, characterized as a fast I/N transition process, followed by a more gradual increase in the birefringence, characterized as a slow I/N transition process. Furthermore, it is quite clear that, with increasing isothermal temperature, the fast I/N transition process is more suppressed, but the slow process is more developed. The polarization of the nematic director changes so rapidly during the thermal equilibration process that stabilized readings cannot be attained, which accounts for the absence of data in the initial stages of the experiment.

A corresponding change of the flowed Schlieren texture with respect to time at constant temperature can be clearly observed, as shown in *Figure 4* for PAME($n=4$), as an example. *Figure 4a* shows the sample quickly quenched to 462.5 K from its isotropic state, and isothermally held at that temperature for 15 s. *Figure 4b* is the same sample under the same isothermal condition, but held for 3 h. It is quite evident that the disclination density changes with respect to isothermal time in addition to the various topological types of disclinations.

If one disregards the fast transition process, an Avrami plot can still be carried out for the PAMEs. *Figure 5*, as an example, shows such plots for PAME($n=3$). One can clearly observe very low Avrami exponent n at all isothermal temperatures. With increasing temperature, furthermore, the value of the exponent n increases from 0.13 at $T_c=475$ K to 0.61 at $T_c=500$ K.

Non-isothermal experiments. Non-isothermal results for PAMEs($n=2$, 3 and 4) are shown in *Table 2*. As previously stated[3], the PAME($n=2$) samples showed negligible degrees of supercooling. They also show little thermal history dependence for the enthalpy of transition, the temperature of transition and the peak half-width during the transition. As the flexible spacer length increases beyond $n=2$, all of these properties show an increasing dependence on cooling rate. For PAME($n=3$), as shown in *Table 2*, the enthalpy of transition, the onset temperatures of T_c and T_d as well as the peak temperatures decrease slightly with increasing cooling or heating rate. The difference between onset temperatures during cooling and heating is about 1–1.5 K, and the difference between peak temperatures during cooling and heating is about 4–9.5 K in a heating and cooling rate range of 5–40 K min^{-1}. The peak half-width is also slightly

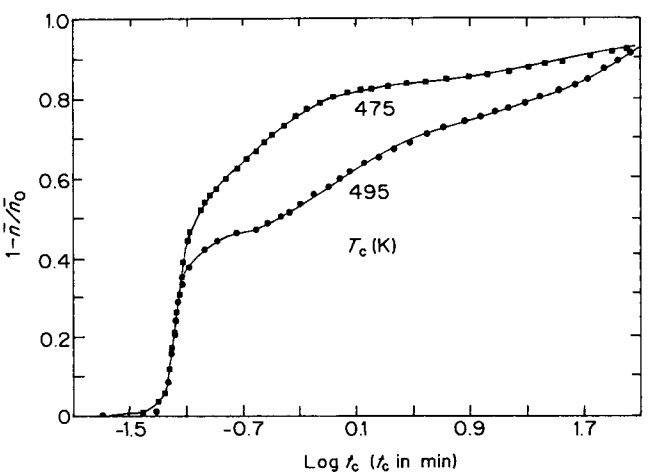

Figure 3 Relationship between the relative intensity change of birefringence and logarithmic annealing time for PAME($n=3$) at 475 and 495 K

Table 2 Non-isothermal transition properties of PAMEs in the region of I/N transitions

Cooling rate (K min^{-1})	ΔH_c (kJ mol^{-1})	ΔH_i (kJ mol^{-1})	T_c(onset) (K)	T_i(onset) (K)	T_c(peak) (K)	T_i(peak) (K)	ΔT_1[a] (K)	ΔT_2[b] (K)	$\Delta T_c^{(1/2)}$ (K)	$\Delta T_i^{(1/2)}$ (K)
$n=2$										
5	1.88	1.88	557.6	557.6	556.0	561.5	0	5.5	4.6	5.3
10	1.86	1.86	557.5	557.5	555.8	561.4	0	5.6	4.9	5.3
20	1.87	1.86	557.3	557.5	555.6	561.3	~0	5.7	5.4	5.3
40	1.86	1.87	557.2	557.5	555.5	561.4	~0	5.9	5.9	5.7
$n=3$										
5	1.99	1.97	508.9	509.9	507.7	512.1	1.0	4.4	3.3	3.5
10	1.97	1.96	508.7	509.8	507.5	512.1	1.1	4.6	3.5	3.6
20	1.96	1.95	508.1	509.2	506.2	513.1	1.1	6.8	5.5	4.5
40	1.88	1.89	507.8	508.7	504.9	514.0	1.2	7.1	6.5	5.6
$n=4$										
5	1.92	2.02	459.7	462.2	461.6	465.7	2.5	4.1	3.9	3.6
10	1.70	1.88	456.5	459.5	457.8	464.0	3.0	6.2	4.3	3.9
20	1.61	1.64	453.0	456.4	452.3	462.5	3.4	10.2	5.7	5.4
40	1.45	1.58	449.0	453.1	444.2	460.9	4.1	16.7	7.1	6.4

[a] $\Delta T_1 = T_i(\text{onset}) - T_c(\text{onset})$
[b] $\Delta T_2 = T_i(\text{peak}) - T_c(\text{peak})$

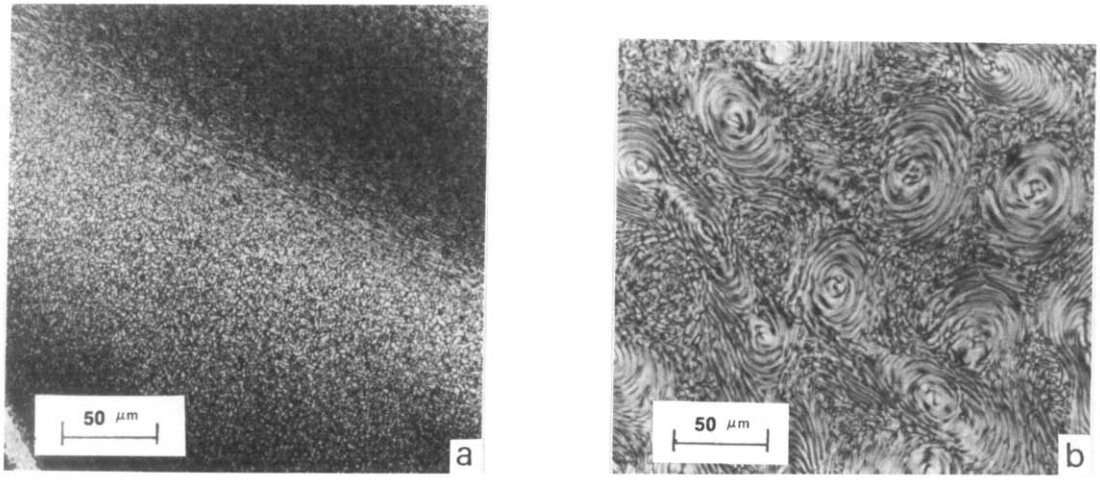

Figure 4 Change of liquid-crystalline textures under p.o.m. for PAME($n=4$) at an isothermal temperature of 462.5 K at different annealing times: (a) right after quenching from its isotropic state; (b) after isothermally annealing for 3 h

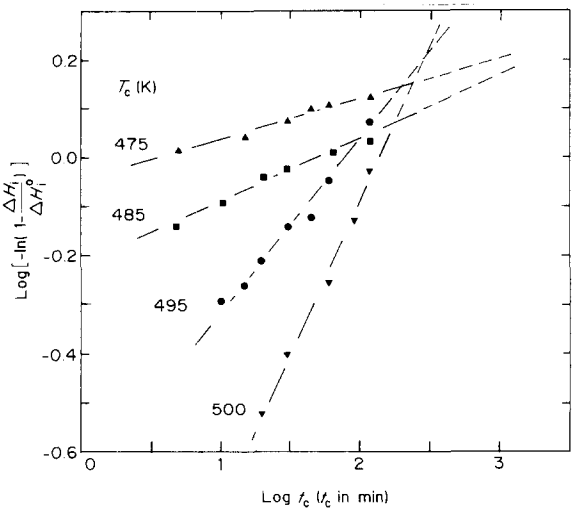

Figure 5 An Avrami plot for the I/N transition of PAME($n=3$) at different isothermal temperatures. Only the slow transition process can be fitted into this equation (see text)

rate-dependent, and is in the range 3.3–6.5 K. A stronger rate-dependent tendency can be observed in the case of PAME($n=4$), as also listed in *Table 2*. The enthalpy of transition now changes by about 25%. The onset temperatures of T_c and T_d change by about 10 K. The peak temperatures change even more, by about 15 K. The difference between onset temperatures during cooling and heating in this case is 2.5–4 K, and the difference between peak temperatures during cooling and heating is 4–17 K. Finally, the peak half-width increases from about 3.5 K to 7.1 K in a heating and cooling rate range of 5–40 K min^{-1}.

Kinetics of N/C transitions

Isothermal experiments. Since PAME($n=1$) decomposes at a temperature lower than its N/I transition temperature, only its N/C transition is examined. The data for the PAME($n=1$) in isothermal experiments can be fitted to an Avrami plot as shown in *Figure 6*. With increasing isothermal temperature, one can find a decrease of the values of both n (from 3.80 at 520 K to 2.40 at 530 K) and K. When the relative enthalpy of transition, $\Delta H_d/\Delta H_d(\text{max})$, reaches about 15–25%, a second process starts, and it leads to a gentler increase in the Avrami plot. The transition that occurs in this isothermal temperature range is very fast. The first process ends after about 1 min at 520 K, and after about 4 min at 530 K. *Figure 7* shows a typical crystalline texture of PAME($n=1$) crystallized at 525 K from its nematic state.

Non-isothermal experiments. The N/C transition of PAME($n=1$) is non-isothermal experiments shows a large supercooling between crystallization and melting of the crystals. *Table 3* lists the data for this transition performed at different cooling rates. It is quite evident that both supercoolings represented by T_d(onset) and T_d(peak) increase with cooling rate, as well as both peak half-widths during heating and cooling. The enthalpy of transition, on the other hand, decreases on increasing the cooling rate.

'Structure recovery' in glass transition region

Isothermal annealing experiments were carried out below the glass transitions of PAMEs at different pre-fixed periods of time and temperature after the samples were quenched rapidly from their nematic or isotropic states. *Figure 8* shows a series of d.s.c. traces for PAME($n=2$), as an example, at $T_a=295$ K. One can see that for short-time annealing (0.75 h) an endothermic peak can be observed before the main glass transition temperature appears. With increasing annealing time, the peak temperature shifts to a higher location and the enthalpy of the peak increases. One small endothermic peak can be seen after the main glass transition, but its temperature and enthalpy are independent of the annealing time and temperature. *Figure 9* illustrates the relationship between the enthalpy of the peak, $\Delta H(t_a, T_a)$, and logarithmic annealing time, log t_a, at $T_a=295$ K for PAME($n=2$) after the samples were quenched from both nematic and isotropic states. Of special interest is the initial development in the enthalpy of the peak for samples quenched from the isotropic state, which is definitely much faster than that for the samples quenched from the nematic state. Only after long-time annealing do the values for the enthalpy of the peak obtained from different quenching states merge. An initial difference of the peak temperatures between the samples quenched from different states can also be observed. Similar observations can also be obtained in the other PAMEs, such as PAME($n=3$ and 4). In the case of PAME($n=1$), we could not carry out this type of experiment due to the fast cold-crystallization process of this polymer, which occurs only a few degrees above the end temperature of the glass transition region. Hence at long annealing, the enthalpy recovery peak would be smeared into the crystallization process.

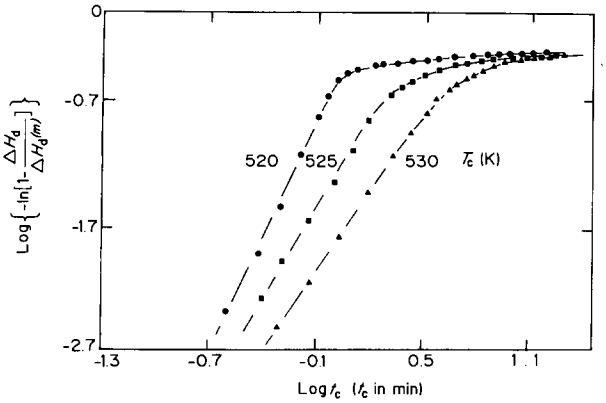

Figure 6 An Avrami plot for the N/C transitions of PAME($n=1$) at different isothermal temperatures

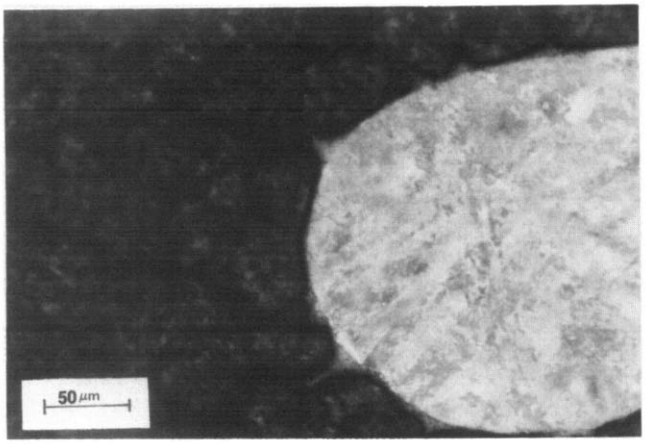

Figure 7 Crystalline texture observed via p.o.m. for PAME($n=1$) crystallized from its nematic state. The isothermal temperature is 473 K

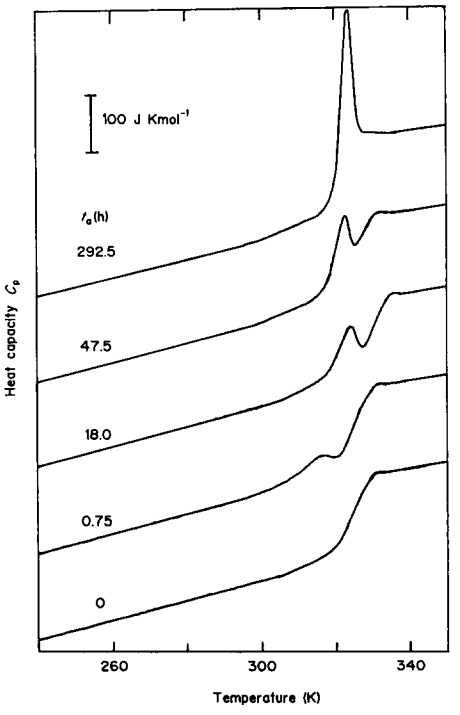

Figure 8 D.s.c. traces of the isothermal annealing experiments at 295 K below its T_g for PAME($n=2$) at different annealing times

Table 3 Non-isothermal transition properties of PAME($n=1$) in the region of its N/C transition

Cooling rate (K min^{-1})	ΔH_c (kJ mol^{-1})	ΔH_d (kJ mol^{-1})	T_c(onset) (K)	T_d(onset) (K)	T_c(peak) (K)	T_d(peak) (K)	ΔT_1[a] (K)	ΔT_2[b] (K)	$\Delta T_c^{(1/2)}$ (K)	$\Delta T_d^{(1/2)}$ (K)
5	28.3	28.9	522.0	548.0	519.0	552.0	26.0	32.5	3.8	6.1
10	26.1	27.2	520.5	546.2	517.0	552.5	25.7	35.5	4.5	7.0
20	25.4	25.5	518.5	544.5	514.0	553.5	26.0	39.5	4.5	9.8
40	24.1	24.0	516.0	541.8	511.0	555.2	25.8	44.2	6.5	11.2

[a] $\Delta T_1 = T_d$(onset) $- T_c$(onset)
[b] $\Delta T_2 = T_d$(peak) $- T_c$(peak)

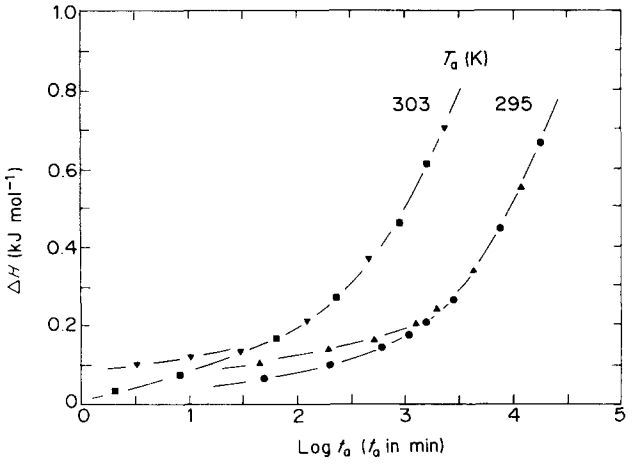

Figure 9 Relationship between the enthalpy of the peak and logarithmic annealing time at $T_a = 295$ and 303 K for PAME($n=2$) after the samples were quenched from both nematic and isotropic states

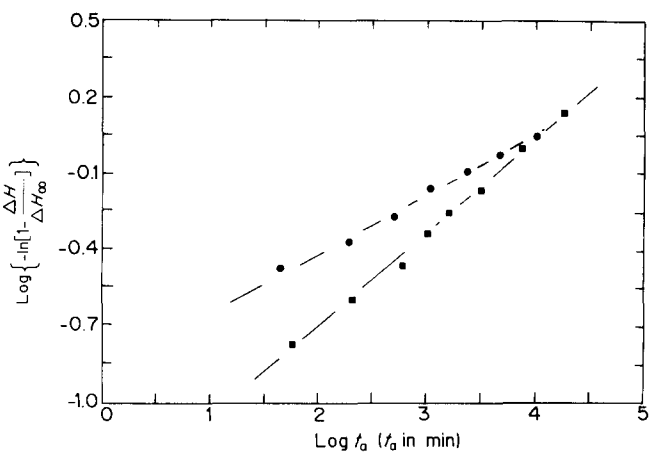

Figure 10 Relationship between $\log[-\ln(1-\Delta H/\Delta H_\infty)]$ and logarithmic annealing time at $T_a = 295$ K as described by equation (3) (see text). ●, Quenched from the isotropic state; ■, quenched from the nematic state

Table 4 Enthalpy relaxation data for PAMEs

n	ΔH_∞[a] (kJ mol^{-1})	T_a (K)	ΔT[b] (K)	β_{iso}[c]	β_{nem}[c]	τ_{iso}[c] (min)	τ_{nem}[c] (min)
2	0.891	295	18	0.244	0.369	4.6×10^3	8.08×10^3
		303	10	0.351	0.517	4.09×10^2	6.12×10^2
3	1.195	250	55	0.111	0.171	5.91×10^5	5.95×10^5
4	1.414	273	20	0.284	0.371	3.22×10^3	5.22×10^3

[a] The values of ΔH_∞ are extrapolated via relationship between $(\Delta H)^{-1}$ and $(t_a)^{-1}\to 0$
[b] The undercooling $\Delta T = T_g - T_a$
[c] The abbreviations iso and nem indicate that the samples were quenched from isotropic and nematic states, respectively. The physical meanings of β and τ are given in equation (3), and see text

If one extrapolates to an infinite annealing time ($1/t_a \to 0$) with respect to the reciprocal of the enthalpy for the peak, $(\Delta H)^{-1}$, for enthalpy of relaxation at equilibrium, ΔH_∞, can be obtained. For PAME($n=2$), the value of ΔH_∞ is 0.891 kJ mol^{-1}, that of PAME($n=3$) is 1.195 kJ mol^{-1} and that of PAME($n=4$) is 1.414 kJ mol^{-1}. They are independent of the annealing temperature. One may consider that the enthalpy relaxation can be expressed by[7,18]:

$$\Delta H(t_a) = \Delta H_\infty[1-\phi(t_a)] \quad (1)$$

where $\phi(t_a)$ is the so-called 'recovery function'. This function is usually further represented to fit the equation[19]:

$$\phi(t_a) = \exp[-(t_a/\tau)^\beta] \quad (2)$$

where τ is the characteristic relaxation time and β is a parameter reflecting the width of the relaxation-time spectrum. Substituting equation (2) into equation (1), and after taking double logarithms and rearranging, one has:

$$\log[-\ln(1-\Delta H/\Delta H_\infty)] = \beta \log t_a - \beta \log \tau \quad (3)$$

Therefore, a plot of $\log[-\ln(1-\Delta H/\Delta H_\infty)]$ vs. $\log t_a$ should demonstrate a linear relationship with a slope of β and an intersection of $\beta \log \tau$. *Figure 10* shows, indeed, such a linear relationship between these two variables for the PAME($n=2$) samples annealed at 295 K. Again, the samples quenched from the nematic state show a higher value for the slope β, and a lower value of $\log \tau$. Several parameters for PAMEs($n=2$, 3 and 4) under different annealing conditions are listed in *Table 4*.

DISCUSSION

It is very interesting to note that in this study of structural formation we have managed to observe the kinetics of I/N transitions for the PAMEs($n=3$ and 4). From *Figures 1–5* and *Table 2* one can understand the following. First, there are two distinguishable transition processes: one occurs very fast (within a few seconds) during quenching through its I/N transition temperature; and another develops gradually later during annealing. Secondly, the fast transition process is characterized by a texture of high disclination density if the supercooling $\Delta T = T_i - T_c$ is large. This process will be suppressed by the following slow transition process when the supercooling becomes small. Thirdly, the slow transition process is increasingly dependent upon the decrease in supercooling. On increasing the annealing time, the disclination density decreases. Finally, such kinetic phenomenon become increasingly prominent when increasing the number of flexible spacers. In fact, the two transition processes in the I/N transition region have been reported in small-molecule liquid crystals by Stein *et al.*[5] and Price *et al.*[6].

Of special importance is the understanding of the physical origins of such observed kinetic phenomena. From our optical observation, the high disclination density forms in the fast transition process, indicating that there are considerably abrupt changes in the trajectories of the directors (different types of disclinations were classified by Frank[20]). These disclinations are static if the supercooling is large. Our d.s.c. measurements also

reveal that the enthalpy of transition at large supercooling has a very minor increase. However, when the temperature approaches T_i (decreasing ΔT), the high disclination density formed in the fast transition process cannot be fully developed, and the disclinations also tend to become mobile, and these disclinations of opposite signs seem to attract one another and coalesce. They may then disappear altogether or form a new singularity. This process can be recognized as the slow transition process, and from our d.s.c. results one can find a large increase in the enthalpy of transition with annealing time. A similar observation has recently been reported by Keller's group in a nematic polyether[21] and in Stein's group in a nematic polyester[22]. One may relate the disclination density to domain size of the nematic states, and a reciprocal correlation between these two variables can be expected. Furthermore, one can also obtain the orientational correlation length since it is assumed that within one domain the mesogenic group orientation is more or less in one direction. We can thus connect such kinetic phenomena with domain growth during the I/C transition in the case of PAMEs. The fast transition process induces aggregation of the chains to form a high domain density. The slow transition process at large supercooling refers mainly to a rearrangement of the orientational order within the domains, and at low supercooling represents additionally the domain growth mechanism. Therefore, in principle, the kinetic phenomena we observed during the I/N transitions are annealing kinetics. This is also indicated by a very low Avrami parameter n for the slow transition process.

Further supporting evidence comes from the difference in the initial development of enthalpy relaxation in the glass transition region for the PAMEs. The samples quenched from their isotropic states cannot bypass their nematic states. However, the enthalpy relaxation for these samples is faster than for those quenched from their nematic states, revealing the different degrees of perfection in the nematic state (see below).

The transition from nematic to crystal state for PAME($n=1$) seems to be a normal crystallization process controlled by nucleation. The only point we would like to emphasize is how fast the transition is if orientational order (even if such order is very imperfect) already exists.

Turning to the LC glass transition region, our isothermal experiments below their main glass transition temperatures provide further evidence for the theoretical predictions suggested by Kovacs *et al.*[7]. We have applied the approach that was reported by Yoshida *et al.*[23]. In fact, the Williams–Watts function[24] represented in equation (2) has been extensively used in describing various relaxation phenomena, such as dielectric, mechanical and dynamic light scattering in polymer systems. The relationship among $\Delta H(t_a, T_a)$, t_a and T_a can eventually be able to predict the annealing characteristics of the PAME LC glasses at any annealing temperature and time. A very interesting mathematical expression is equation (3). The equation is apparently very similar to an Avrami equation. This again indicates that without parallel knowledge of the microscopic, independently proven mechanism, the macroscopic, experimentally derived Avrami equation is only a convenient means to represent empirical data. We have used equation (3) to treat our enthalpy relaxation data, which is obviously different from polymer crystallization.

On the other hand, our values of β and τ reveal, indeed, the proper tendency for enthalpy relaxation. The value of β for samples quenched from the isotropic state is smaller than that for samples quenched from the nematic state, indicating that the relaxation-time spectrum for the former process is broader than that of the latter. At the same time, the characteristic relaxation time τ for the former process is lower than its counterpart for the nematic quenched samples. Presumably this difference should decrease in magnitude on increasing the number of flexible spacers, as indicated in the cases of PAME($n=2$) at an undercooling ($T_g - T_a$) of 18 K and PAME($n=4$) at an undercooling of 20 K in *Table 4*.

It is also very interesting to relate our isothermal experiments to the hysteresis experiment we reported in our previous paper where the hysteresis observations were studied under non-isothermal conditions. An experiment carried out isothermally at a long annealing time is equivalent to the hysteresis observation at a very slow cooling rate. There must certainly be a correlation between these two types of relaxation behaviour. It is our goal to establish such a correlation in polymeric glassy states.

CONCLUSIONS

The phase transitions of a series of PAMEs have been studied. Evidence has been presented for the structural formation kinetics in PAMEs. This paper can be evaluated from the following points.

The I/N transition for PAMEs($n=2$, 3 and 4) was found to proceed by two processes: a fast process followed by a slow structure-sensitive process, which develops on annealing. The slow process is greatly enhanced by increasing the number of flexible spacers. Isothermal experiments reveal that the peak half-widths during the transition decrease exponentially with annealing time. This effect is increasingly pronounced as the annealing temperature is increased. In addition, the enthalpies of transition become progressively more dependent upon annealing time as the number of flexible spacers is increased. Non-isothermal experiments reveal that the enthalpy of transition, temperature of transition and peak half-width during the transition show an increasing dependence upon cooling rate. A stronger dependence is found on increasing the number of flexible spacers.

Coupling d.s.c. measurements with p.o.m. observations, one finds that the fast process is linked to a texture of high disclination density, whereas the slow process involves the transformation of these disclinations into a higher-order singularity. This can in turn be representative of the domain size. This information can also be recognized as the observed increase in enthalpy of transition with annealing time.

The N/C transition for PAME($n=1$) was found to follow normal nucleation and growth steps.

Isothermal experiments in LC glass transition regions have shown that the relaxation spectra for samples quenched from their isotropic states relax an order of magnitude faster than those for samples quenched from their nematic states, which then later merge. Presumably this behaviour decreases in magnitude on increasing the number of flexible spacers. Application of the enthalpy relaxation model expressed in the form of equation (3) has enabled us to extract out the characteristic parameters of the relaxation process.

A possible correlation indeed exists between non-isothermal experiments (hysteresis) and isothermal experiments (structure recovery) in the glass transition region.

ACKNOWLEDGEMENT

This work was partially supported by the Research Challenge Grant of Ohio State Regent through the University of Akron.

REFERENCES

1 Morgan, P. W., Kwolek, S. L. and Pletcher, T. C. *Macromolecules* 1987, **20**, 729
2 Harris, F. W. and Sridhar, K. *Polym. Prepr., Am. Chem. Soc., Div. Polym. Chem.* 1988, **29** (2), 304
3 Cheng, S. Z. D., Janimak, J. J., Sridhar, K. and Harris, F. W. *Polymer* 1989, **30**, 494
4 Wunderlich, B. and Grebowicz, J. *Adv. Polym. Sci.* 1984, **60/61**, 1
5 Jabarin, S. A. and Stein, R. S. *J. Phys. Chem.* 1973, **77**, 409
6 Price, F. P. and Wendorff, J. H. *J. Phys. Chem.* 1971, **75**, 2938; 1971, **75**, 2849; 1972, **76**, 276; Price, F. P. and Fritzsche, A. K. *J. Phys. Chem.* 1973, **77**, 409
7 Kovacs, A. J., Aklonis, J. J. and Hutchinson, J. M. *J. Polym. Sci., Polym. Phys. Edn.* 1979, **17**, 1097, 2031; Ramos, A. R., Hutchison, J. M. and Kovacs, A. J. *J. Polym. Sci., Polym. Phys. Edn.* 1984, **22**, 1655; Ramos, A. R., Kovacs, A. J., O'Reilly, J. M., Tribone, J. J. and Greener, J. *J. Polym. Sci., Polym. Phys. Edn.* 1988, **26**, 501
8 Weitz, A. and Wunderlich, B. *J. Polym. Sci., Polym. Phys. Edn.* 1974, **12**, 2473
9 Petrie, S. E. B. *J. Macromol. Sci., Phys.* (*B*) 1976, **12**, 225
10 Petrie, S. E. B. *J. Polym. Sci.* (*A-2*) 1972, **10**, 1255
11 Brown, I. G., Wetton, R. E., Richardson, M. J. and Savill, N. G. *Polymer* 1978, **19**, 659
12 Ali, M. S. and Sheldon, R. O. *J. Appl. Polym. Sci.* 1970, **14**, 2619
13 Ott, H. *Colloid Polym. Sci.* 1979, **257**, 486
14 Wysgoski, M. G. *J. Appl. Polym. Sci.* 1980, **25**, 1455
15 Gray, A. and Gilbert, M. *Polymer* 1976, **17**, 44
16 Foltz, C. R. and McKinney, P. V. *J. Appl. Polym. Sci.* 1969, **13**, 2235
17 Wunderlich, B. and Bopp, R. C. *J. Thermal. Anal.* 1974, **6**, 635; see also Mehta, A., Bopp, R. C., Gaur, U. and Wunderlich, B. *J. Thermal. Anal.* 1978, **13**, 197
18 Ruddy, M. and Hutchinson, J. M. *Polym. Commun.* 1988, **29**, 132
19 Cowie, J. M. G. and Ferguson, R. *Polym. Commun.* 1986, **27**, 258
20 Frank, F. C. *Discuss. Faraday Soc.* 1958, **25**, 19
21 Feijoo, J. L., Unger, G., Owen, A. J., Keller, A. J. and Percec, V. *Mol. Cryst. Liq. Cryst.* 1988, **155**, 487
22 Rojstaczer, S., Goldman, E. and Stein, R. S. *Bull. Am. Phys. Soc.* 1989, **34**, 524
23 Yoshida, H. and Kobayashi, Y. *J. Macromol. Sci., Phys.* (*B*) 1982, **31**, 565
24 Williams, G. and Watts, D. C. *Trans. Faraday Soc.* 1970, **66**, 80